

# XV Latin American Symposium on High Energy Physics

November 4 - 8, 2024, Cinvestav, Mexico city



Cinvestav



SOCIEDAD MEXICANA DE FÍSICA



Instituto de  
Física  
UNAM

**Improved  $\pi^0$ ,  $\eta$  and  $\eta'$  transition form factors**

in  $R\chi T$  and their  $a_\mu^{HLbL}$  contribution

---

Emilio J. Estrada ([emilio.estrada@cinvestav.mx](mailto:emilio.estrada@cinvestav.mx))

EJE, S. González-Solís, A. Guevara, P. Roig arXiv:2409.10503v1

SILAAE XV, November 4 - 8, 2024, Mexico City

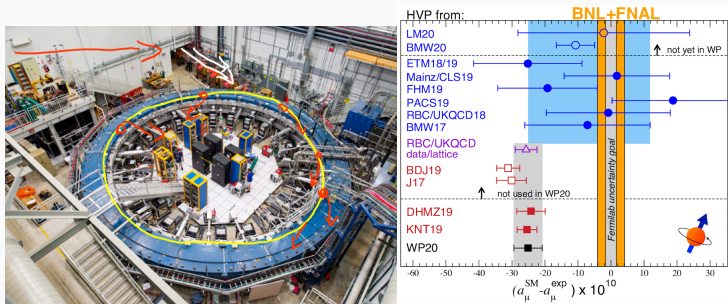
# Table of contents

1. Motivation
2. An  $R_\chi T$  description of the TFFs
3. Form factor data analysis
4. Results
5. Conclusions

## Motivation

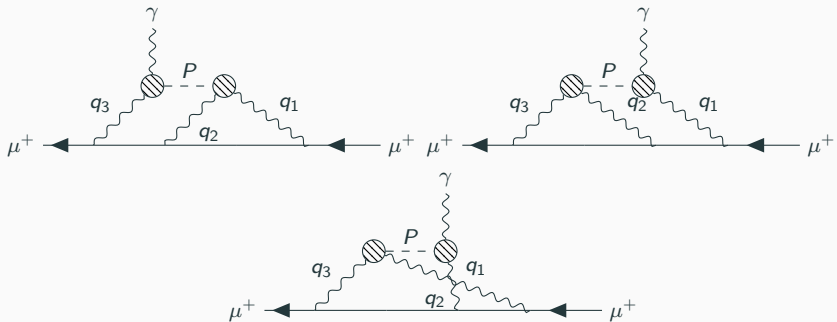


The different experimental results come from BNL('04) and FNL runs 1, 2 and 3 and are in a  $5.1\sigma$  tension with respect to the theory initiative White Paper (Phys.Rept. 887 (2020) 1-166). The main challenge are the hadronic contributions. Particularly HVP now, and also HLbL (our focus today) for near-future precision.



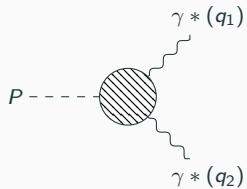
## HLbL piece of $a_\mu$ : P-pole contribution

$g - 2$  requires an improvement on the theoretical hadronic sector where the transition form factors are an essential input of a relevant contribution. New experimental data and lattice QCD descriptions can be used to fit the parameters of a  $R\chi T$  model with two vector meson multiplets.



Feynman diagrams for the pseudoscalar-pole contribution to the HLbL piece of  $a_\mu$ .

We construct these form factors for general values of the virtualities of the two photons,  $q_1$  and  $q_2$ , using a two-hadron multiplet saturation scheme under Chiral Perturbation Theory ( $\chi PT$ ).



$$\mathcal{M}_{P\gamma^*\gamma^*} = ie^2 \epsilon^{\mu\nu\rho\sigma} q_{1\mu} q_{2\nu} \epsilon_{1\rho}^* \epsilon_{2\sigma}^* \mathcal{F}_{P\gamma^*\gamma^*}(q_1^2, q_2^2).$$

Challenge: QCD is not perturbative below 2 GeV, Low energy EFT covers only below 1 GeV.

For the HLbL diagrams of the P-poles, its  $a_\mu$  contribution is computed as:

$$a_\mu^{\text{P-pole}} = -\frac{2\alpha^3}{3\pi^2} \int_0^\infty dQ_1 dQ_2 \int_{-1}^1 dt \sqrt{1-t^2} Q_1^3 Q_2^3 [F_1 P_6 I_1(Q_1, Q_2, t) + F_2 P_7 I_2(Q_1, Q_2, t)] ,$$

where  $\alpha$  is the fine structure constant,  $Q_i = |Q_i|$ ,  $t = \cos \theta$ ,  $P_6 = \frac{1}{Q_2^2 + m_\gamma^2}$ ,

$P_7 = \frac{1}{Q_3^2 + m_P^2}$ ,  $Q_3^2 = Q_1^2 + Q_2^2 + 2Q_1 Q_2 t$  and the  $I_{1(2)}(Q_1, Q_2, t)$  are given in A.

Nyffeler, Phys. Rev. D 94 (2016) 053006, 1602.03398. The information of the transition form factors is encoded in:

$$F_1 = \mathcal{F}_{P\gamma^*\gamma^*}(Q_1^2, Q_3^2) \mathcal{F}_{P\gamma^*\gamma}(Q_2^2, 0) .$$

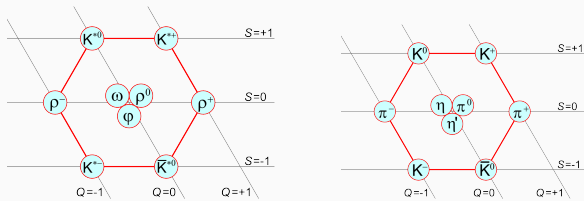
$$F_2 = \mathcal{F}_{P\gamma^*\gamma^*}(Q_1^2, Q_2^2) \mathcal{F}_{P\gamma^*\gamma}(Q_3^2, 0) .$$

## An $R\chi T$ description of the TFFs

---

# Our Building Blocks

A mass spectrum:



A phenomenological symmetry-based model at NLO in chiral counting:

$$\begin{aligned}\mathcal{L} = & \mathcal{L}_{\text{non-R}} + \mathcal{L}_V^{\text{Kin}} + \mathcal{L}_V^{\text{EM interactions}} + \mathcal{L}_{VV}^{\text{EM interactions}} + \mathcal{L}_P, \\ & + (V \rightarrow V') + \mathcal{L}_{VV'}^{\text{EM interactions}} + \mathcal{L}_{P'VV'}\end{aligned}$$

We will demand that our form factors, satisfy the high-energy (SDCs) requirements stemming from pQCD:

$$\lim_{Q^2 \rightarrow \infty} -Q^2 \mathcal{F}_{\pi^0 \gamma^* \gamma^*}(-Q^2, -Q^2) = \frac{2F_\pi}{3},$$

$$\lim_{Q^2 \rightarrow \infty} -Q^2 \mathcal{F}_{\pi^0 \gamma^* \gamma^*}(-Q^2, 0) = 2F_\pi,$$

with  $q^2 = -Q^2$ . Besides,  $\langle VVP \rangle$  asymptotic constraints will be imposed, in both chiral ( $m_P^2$ ) and momentum ( $Q^2$ ) counting.

The ratio between the asymptotic constraints  $\pi:\eta:\eta'$  is given in terms of the mixings between the flavor and the mass basis -these mixings are parametrized by two angles  $\theta_{0(8)}$  and two decay constants  $f_{0(8)}$ :

$$1 : \left( \frac{5C_q - \sqrt{2}C_s}{3} \right) : \left( \frac{5C'_q + \sqrt{2}C'_s}{3} \right)$$

## **Form factor data analysis**

---

After imposing SDCs, 12 free parameters remain, 3 mass parameters ( $M_V$ ,  $e_m^V$ ,  $M_{V'}$ ), 5 linear combinations of the coupling constants<sup>1</sup> and the 4 mixing parameters. These were fitted to:

- The decay widths  $\Gamma(P \rightarrow \gamma\gamma)$ , related to  $\mathcal{F}_{P\gamma\gamma}$  (real photons) as

$$\Gamma(P \rightarrow \gamma\gamma) = \frac{(4\pi\alpha)^2}{64\pi} m_P^3 |\mathcal{F}_{P\gamma\gamma}(0,0)|^2,$$

- TFF data from the BaBar, Belle, CELLO, CLEO, and LEP experiments, for the single virtual case of all 3 P-mesons.
- BaBar TFF doubly virtual data for  $\eta'$ , and LQCD generated data from BMW collaboration for all 3 P-TFFs.
- The subleading asymptotic contribution to double virtual  $\pi^0$ -TFF,  $\delta_\pi^2$ .
- Stabilization points for the parameters of the mixings and the mass parameters.

---

<sup>1</sup>3 of them are sensitive to DV data only.

A global reduced  $\chi^2$  analysis was performed:

$$\chi^2_{\text{Global}} = \chi^2_{\pi_0^{\text{SV}}} + \chi^2_{\eta_{\text{SV}}} + \chi^2_{\eta'_{\text{SV}}} + \chi^2_{\pi_0^{\text{DV}}} + \chi^2_{\eta_{\text{DV}}} + \chi^2_{\eta'_{\text{DV}}} + \sum_P^{\text{ExtraPoints}} \left( \frac{P_{\text{exp}} - P_{\text{model}}}{\Delta P_{\text{exp}}} \right)^2,$$

where the correlation between LQCD data points was taken in consideration:

$$\chi^2_{P_{\text{DV}}^{\text{LQCD}}} = \sum_{i,j=1}^3 \left( P_i^{\text{LQCD}} - P_i^{\text{RxT}} \right) \left( \text{Cov}_{ij}^{\text{LQCD}} \right)^{-1} \left( P_j^{\text{LQCD}} - P_j^{\text{RxT}} \right),$$

## Results

---

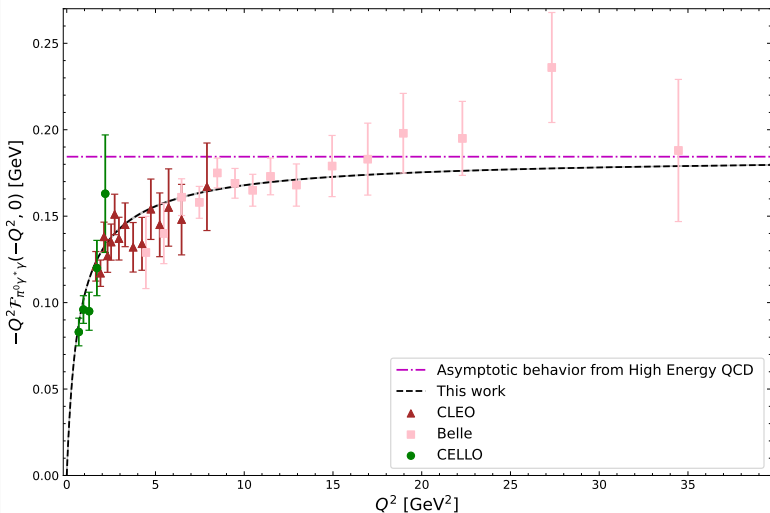
# Global Fit Results

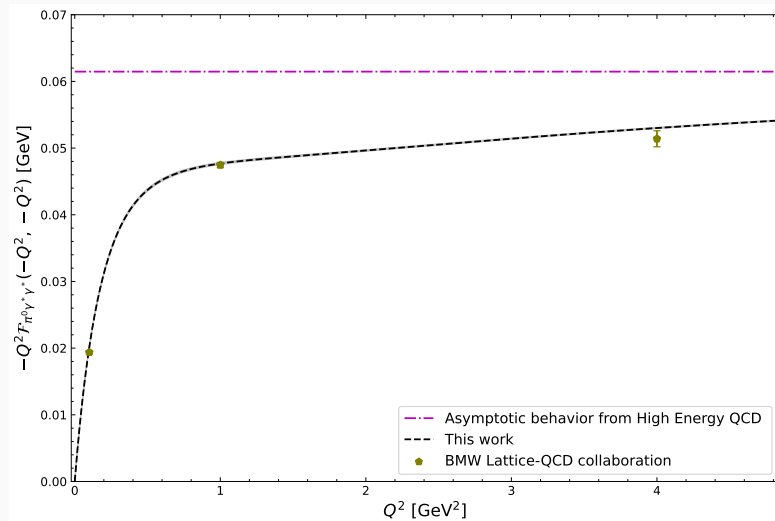
Parameter	GF Value
$M_V$ [GeV]	0.752(2)
$e_m^V$	-0.32(4)
$M_{V'}$ [GeV]	1.933(4)
$r_{s1}$	0.0(0.6)
$r_{s2}$	0.0(0.9)
$r_s$	0.9976
$\theta_8$ [°]	-18.5(6)
$\theta_0$ [°]	-6.9(1.6)
$f_8$ [MeV]	118.8(4)
$f_0$ [MeV]	99.4(1.7)
$r_{d1}$	0.0(0.5)
$r_{d2}$	0.0(0.9)
$r_d$	0.9783
$d_{d3}$	-3.48(3)
$\chi^2_{Global}$ d.o.f.	148.0 110

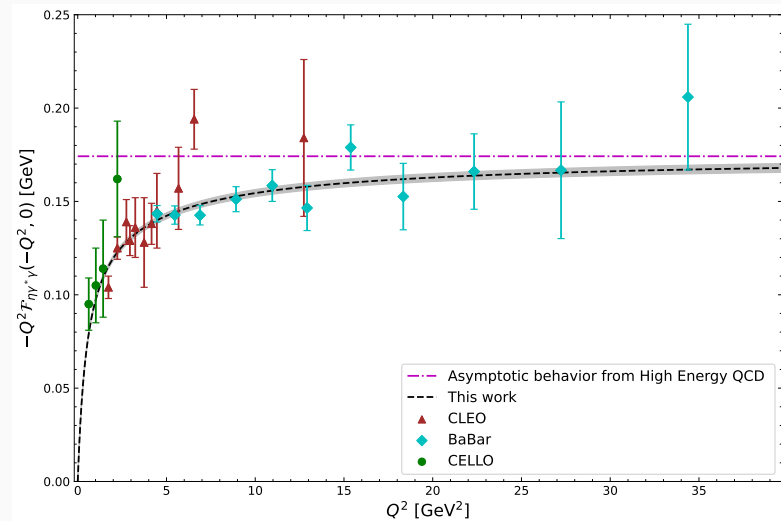
	M_V	evm	M_V2	rs1	rs2	th8	th0	f8	f0	rd1	rd2	dd3
M_V	2.79e-06	5.19e-05 (0.739)	-2.2e-07 (-0.035)	0.000509 (0.501)	-0.000101 (-0.065)	3.52e-05 (0.035)	-2.27e-05 (-0.008)	-4.43e-07 (-0.077)	-7.02e-08 (-0.025)	0.000288 (0.357)	-0.000232 (-0.152)	1.83e-05 (0.371)
evm	5.19e-05 (0.739)	0.00177	-1.67e-05 (-0.106)	0.0157 (0.614)	-0.00472 (-0.120)	-0.000237 (-0.009)	0.00132 (0.019)	-1.43e-05 (-0.099)	-3.69e-06 (-0.053)	0.00612 (0.300)	-0.0056 (-0.145)	0.000427 (0.344)
M_V2	-2.2e-07 (-0.035)	-1.67e-05 (-0.106)	1.43e-05 (-0.035)	-8e-05 (-0.114)	-0.000403 (-0.032)	-7.2e-05 (-0.032)	0.00124 (0.202)	8.15e-07 (0.063)	-1.86e-07 (-0.030)	-0.000817 (-0.446)	0.00138 (0.399)	-9.33e-05 (-0.837)
rs1	0.000509 (0.501)	0.0157 (0.614)	-8e-05 (-0.035)	0.371 (0.226)	0.129 (0.335)	0.123 (0.226)	0.0287 (0.185)	-2.96e-05 (-0.014)	-0.000115 (-0.113)	0.0639 (0.217)	-0.054 (-0.097)	0.00333 (0.186)
rs2	-0.000101 (-0.065)	-0.00472 (-0.120)	-0.000403 (-0.114)	0.129 (0.226)	0.877 (0.185)	0.104 (0.185)	-0.332 (-0.219)	0.000285 (0.089)	0.000672 (0.431)	0.0118 (0.026)	0.181 (0.211)	0.00226 (0.062)
th8	3.52e-05 (0.035)	-0.000237 (-0.009)	-7.2e-05 (-0.032)	0.123 (0.335)	0.104 (0.185)	0.364 (0.185)	0.00228 (-0.219)	-0.00138 (-0.657)	-6.96e-05 (-0.069)	0.0218 (0.075)	0.0392 (0.071)	0.000269 (0.015)
th0	-2.27e-05 (-0.008)	0.00132 (0.019)	0.00124 (0.202)	0.0287 (-0.014)	-0.332 (-0.219)	0.00228 (-0.219)	2.64 (-0.219)	-3.16e-06 (-0.089)	0.00164 (0.605)	-0.0539 (-0.069)	-0.0669 (-0.041)	-0.00889 (-0.187)
f8	-4.43e-07 (-0.077)	-1.43e-05 (-0.099)	8.15e-07 (0.063)	-2.96e-05 (-0.014)	0.000285 (-0.089)	-0.00138 (-0.657)	-3.16e-06 (-0.089)	1.18e-05 (0.032)	1.83e-07 (0.032)	-7.85e-05 (-0.047)	7.83e-06 (0.002)	-8.51e-06 (-0.064)
f0	-7.02e-08 (-0.025)	-3.69e-06 (-0.053)	-1.86e-07 (-0.030)	-0.000115 (-0.113)	0.000672 (0.431)	-6.96e-05 (-0.069)	0.00164 (0.605)	1.83e-07 (0.032)	2.78e-06 (-0.011)	-8.93e-06 (-0.022)	0.000252 (0.165)	1.49e-06 (0.030)
rd1	0.000288 (0.357)	0.00612 (0.300)	-0.000817 (-0.446)	0.0639 (0.217)	0.0118 (0.026)	0.0218 (0.075)	-0.0539 (-0.069)	-7.85e-05 (-0.047)	-8.95e-06 (-0.011)	0.235 (-0.152)	-0.0676 (-0.152)	0.002 (0.140)
rd2	-0.000232 (-0.152)	-0.0056 (-0.145)	0.00138 (0.399)	-0.054 (-0.097)	0.181 (0.211)	0.0392 (0.071)	-0.0609 (-0.041)	7.83e-06 (0.002)	0.000252 (0.165)	-0.0676 (-0.152)	0.843 (-0.140)	-0.0106 (-0.392)
dd3	1.83e-05 (0.371)	0.000427 (0.344)	-9.33e-05 (-0.837)	0.00333 (0.186)	0.00226 (0.082)	0.000269 (0.015)	-0.00898 (-0.187)	-8.51e-06 (-0.084)	1.49e-06 (0.030)	0.002 (0.140)	-0.0106 (-0.392)	0.000871

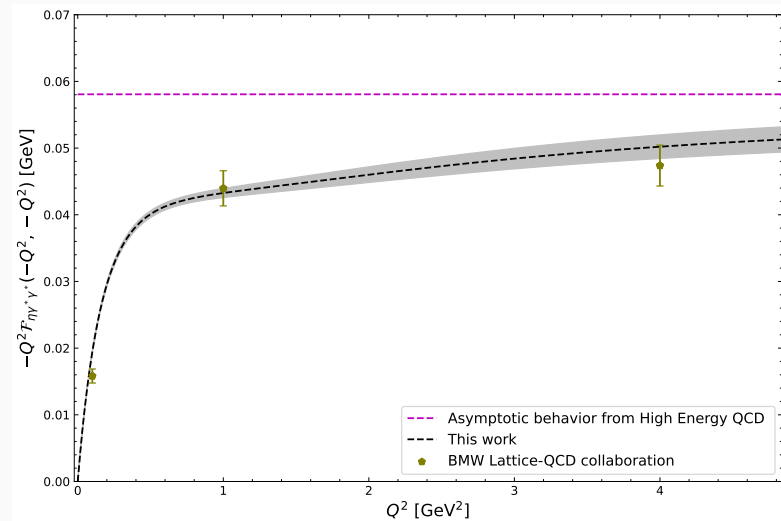
Covariance Matrix of the Fitted Parameters after block diagonalization was performed in both single and double virtual sector.

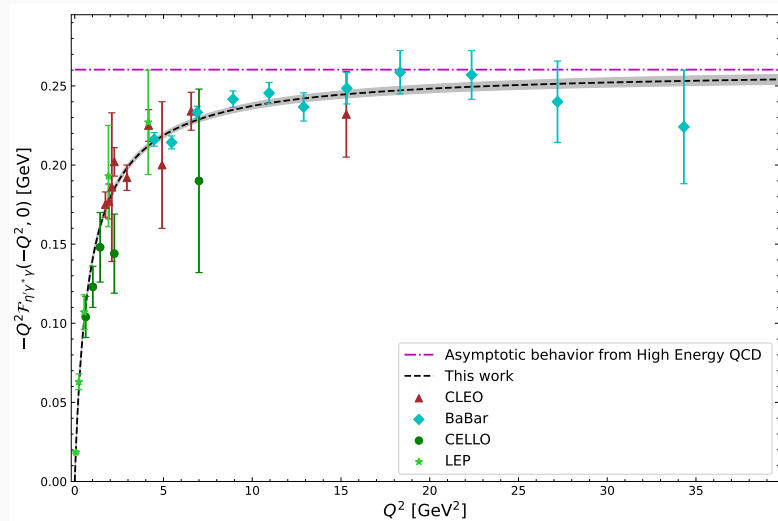
Best fit results

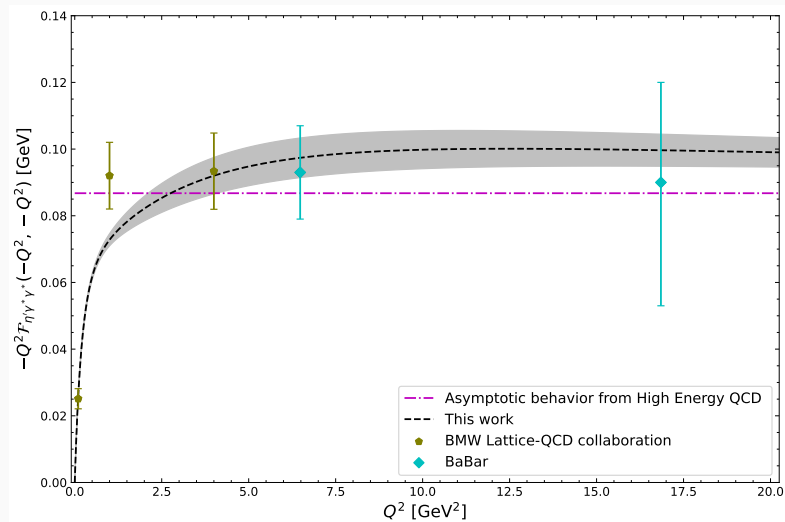


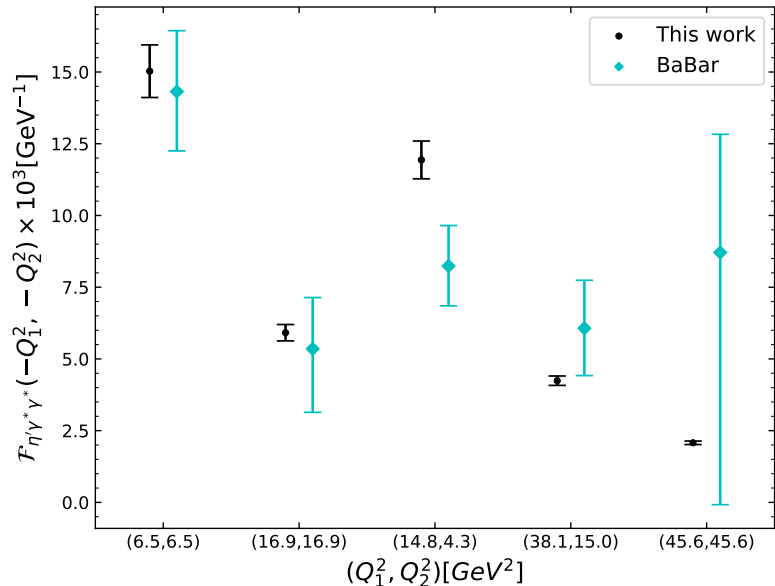








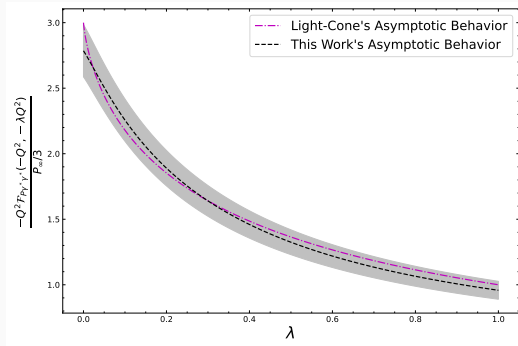




# Asymptotic Behavior: Light-Cone Expansion

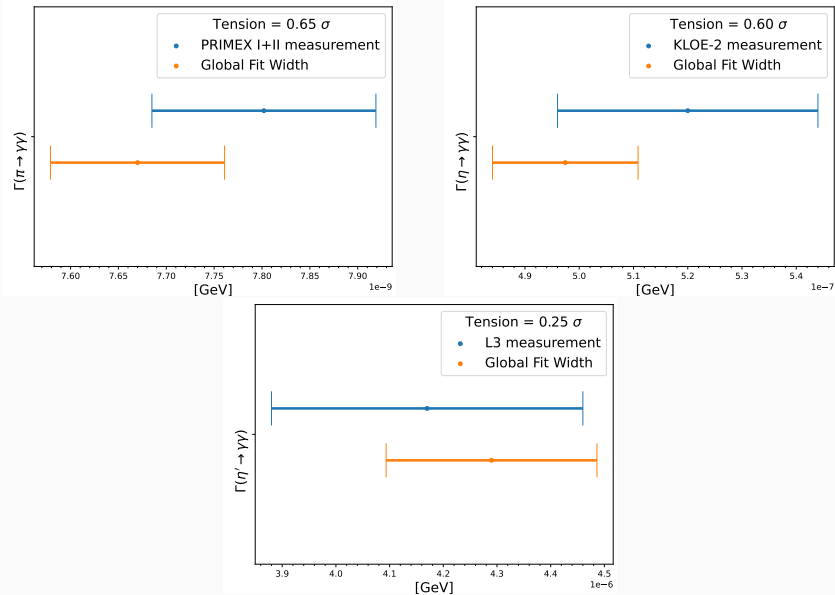
The Light-Cone expansion prescribes a continuum high-energy behavior:

$$\lim_{Q_{1(2)}^2 \rightarrow \infty} \mathcal{F}_{P\gamma^*\gamma^*}(-Q_1^2, -Q_2^2) = \frac{P_\infty}{3} \int_0^1 dx \frac{\phi_P(x)}{xQ_1^2 + (1-x)Q_2^2},$$



This work's vs LCE SDC's

## Low Energy Behavior: $\Gamma(P \rightarrow \gamma\gamma)$



# Assessment of theory uncertainties for $a_\mu^{\text{P-pole}}$

Considered systematic errors  $\times 10^{+11}$

	Data Set	Finite Tower of Resonances	Subleading $1/N_C$	Hybrid Analysis
$\pi^0$	+0.20	+1.8	$\pm 1.5$	+0.4
$\eta$	-0.02	+1.0	$\pm 0.5$	-0.6
$\eta'$	+0.02	+1.4	$\pm 0.3$	-0.8

- Data Set: BaBar was not used
- Finite Tower of Resonances: An EFT based on large- $N_C$  has infinite active d.o.f. but we cut them to 2 multiplets, integrating out the rest.
- Subleading  $1/N_C$ : There are loop corrections to e.g. the V meson propagators.
- Hybrid Analysis: Our work might be biased by LQCD data.

# $a_\mu^{\text{P-pole}}$ Results

$\pi^0$	$\eta$	$\eta'$	Ref.	Method
$63.0^{+2.7}_{-2.1}$	$14.64 \pm 0.77$	$13.44 \pm 0.70$	JHEP 10 (2018) 141 Hofferichter, et al.	Dispersive
$63.6 \pm 2.7$	$16.3 \pm 1.4$	$14.5 \pm 1.9$	PRD 95, 054026 (2017) P. Sánchez-Puertas, Masjuan	CA
$62.6 \pm 1.3$	$15.8 \pm 1.2$	$13.3 \pm 0.9$	PLB 797 (2019) 134855 Eichmann et al.	DS eqs.
$61.4 \pm 2.1$	$14.7 \pm 1.9$	$13.6 \pm 0.8$	PRD 101 (2020) 7, 074021 Raya, Bashir & Roig	DS eqs.
$63.0^{+2.7}_{-2.1}$	$16.3 \pm 1.4$	$14.5 \pm 1.9$	Phys.Rept. 887 (2020) 1-166 Aoyama et al.	WP Data-driven
$62.3 \pm 2.3$	-	-	Phys.Rept. 887 (2020) 1-166 Aoyama et. al. (Gerardin et. al.)	WP Lattice (BMW)
$57.8 \pm 2.0$	$11.6 \pm 2.0$	$15.7 \pm 4.3$	arXiv:2305.04570 Gerardin et. al.	Lattice
$61.7 \pm 2.0$	$13.8 \pm 5.5$	-	PRD 108 (2023) 9 Alexandrou	Lattice
$63.5 \pm 0.8$	-	-	JHEP 03 (2023) 118 Kadavy, Kampf & Novotny	R $\chi$ T, 3 RM
$61.9 \pm 0.6^{+2.4}_{-1.5}$	$15.2 \pm 0.5^{+1.1}_{-0.8}$	$14.2 \pm 0.7^{+1.4}_{-0.9}$	arXiv: 2409.10503 EJE, González-Solís Guevara & Roig	R $\chi$ T 2 RM

Different recent evaluations of  $a_\mu^{\text{P-poles}}$ ,  $P = \pi^0, \eta, \eta'$ , multiplied by  $10^{11}$ .

## **Conclusions**

---

- A correct description of P-TFF at low, intermediate, and high energies was achieved using a  $R\chi T$  model with two multiplets of vector meson resonances.
- We have successfully completed a hybrid analysis that uses LQCD data to complement the scarce data in the doubly virtual sector of the TFFs.
- Chiral Symmetry allows us to complement BaBar data for double virtuality to be used in the fits avoiding overfitting (this is the problem for CAs, the method of the current central value in the WP). As a result we have achieved the best current description of the available data, which is being appreciated by the Theory Initiative.
- Solid computation of the P-pole contributions was achieved together with robust statistical and systematic errors.
- Our evaluation of the pole contributions to the hadronic light-by-light piece of the muon  $g - 2$  read:  $a_{\mu}^{\pi^0\text{-pole}} = (61.9 \pm 0.6^{+2.4}_{-1.5}) \times 10^{-11}$ ,  
 $a_{\mu}^{\eta\text{-pole}} = (15.2 \pm 0.5^{+1.1}_{-0.8}) \times 10^{-11}$  and  $a_{\mu}^{\eta'\text{-pole}} = (14.2 \pm 0.7^{+1.4}_{-0.9}) \times 10^{-11}$ , for a total of  $a_{\mu}^{\pi^0+\eta+\eta'\text{-pole}} = (91.3 \pm 1.0^{+3.0}_{-1.9}) \times 10^{-11}$ , where the first error is statistical and the second one is systematic.

**Thank you!**

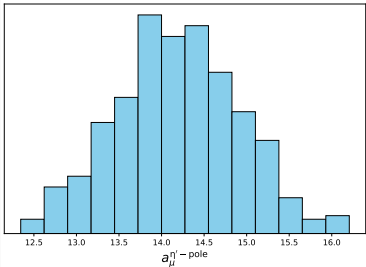
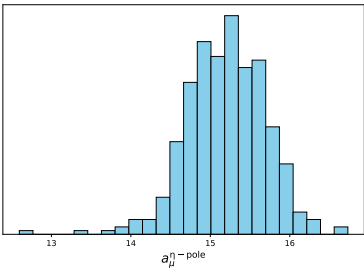
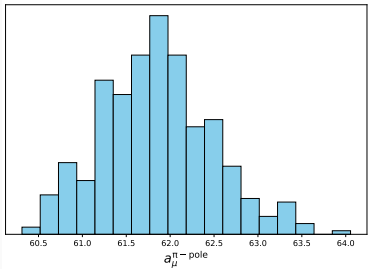
---

## **Backup**

---

## Numerical Evaluation

a total of 1000 points in the parameter space were generated using a multivariate gaussian distribution, considering the mean values and the covariances of the fitted parameters.



# Correlation Matrix before rotation

	M_V	evm	M_V2	ds1	ds2	th8	th0	f8	f0	dd1	dd2	dd3
M_V	2.19e-05	0.000393 (0.947)	0.000105 (0.389)	0.00199 (0.766)	0.000244 (0.747)	-4.19e-05 (-0.014)	0.000652 (0.085)	-2.88e-06 (-0.177)	-8.81e-07 (-0.111)	0.00131 (0.143)	0.00016 (0.140)	-0.00071 (-0.316)
evm	0.000393 (0.947)	0.00788	0.00169 (0.330)	0.0402 (0.815)	0.00493 (0.796)	-0.00107 (-0.019)	0.0137 (0.094)	-5.84e-05 (-0.189)	-1.79e-05 (-0.119)	0.0254 (0.146)	0.00308 (0.142)	-0.0111 (-0.261)
M_V2	0.000105 (0.389)	0.00169 (0.330)	0.00334	-0.000489 (-0.015)	-0.000127 (-0.031)	-0.00789 (-0.218)	0.0013 (0.014)	-1.18e-05 (-0.058)	-5.16e-06 (-0.053)	0.00396 (0.035)	0.000707 (0.050)	-0.0276 (-0.995)
ds1	0.00199 (0.766)	0.0402 (0.815)	-0.000489 (-0.015)	0.309	0.0387 (0.998)	0.0945 (0.271)	0.0998 (0.110)	-0.00025 (-0.129)	-0.000148 (-0.158)	0.171 (0.157)	0.0202 (0.148)	0.0205 (0.077)
ds2	0.000244 (0.747)	0.00493 (0.796)	-0.000127 (-0.031)	0.0387 (0.998)	0.00487	0.0125 (0.286)	0.0109 (0.095)	-2.93e-05 (-0.120)	-1.5e-05 (-0.127)	0.0215 (0.157)	0.00255 (0.149)	0.00307 (0.092)
th8	-4.19e-05 (-0.014)	-0.00107 (-0.019)	-0.00789 (-0.218)	0.0945 (0.271)	0.0125 (0.286)	0.393	0.0209	-0.00135 (-0.615)	-6.65e-05 (-0.063)	0.162 (0.132)	0.0207 (0.135)	0.0643 (0.214)
th0	0.000652 (0.085)	0.0137 (0.094)	0.0013 (0.014)	0.0998 (0.110)	0.0109 (0.095)	0.0209	2.67	-9.41e-05 (-0.017)	0.00163 (0.589)	0.0244 (0.008)	0.00171 (0.004)	-0.00523 (-0.007)
f8	-2.88e-06 (-0.177)	-5.84e-05 (-0.189)	-1.18e-05 (-0.058)	-0.00025 (-0.129)	-2.93e-05 (-0.120)	-0.00135 (-0.615)	-9.41e-05 (-0.017)	1.22e-05	2.97e-07 (0.050)	-0.00023 (-0.034)	-2.86e-05 (-0.033)	7.66e-05 (0.046)
f0	-8.81e-07 (-0.111)	-1.79e-05 (-0.119)	-5.16e-06 (-0.053)	-0.000148 (-0.158)	-1.5e-05 (-0.127)	-6.65e-05 (-0.063)	0.00163 (0.589)	2.97e-07 (0.050)	2.86e-06 (-0.038)	-0.000126 (-0.026)	-1.07e-05 (-0.026)	3.77e-05 (0.046)
dd1	0.00131 (0.143)	0.0254 (0.146)	0.00396 (0.035)	0.171 (0.157)	0.0215 (0.157)	0.162 (0.132)	0.0244 (0.008)	-0.00023 (-0.034)	-0.000126 (-0.038)	3.84	0.478 (0.997)	-0.0833 (-0.089)
dd2	0.00016 (0.140)	0.00308 (0.142)	0.000707 (0.050)	0.0202 (0.148)	0.00255 (0.149)	0.0207 (0.135)	0.00171 (0.004)	-2.86e-05 (-0.033)	-1.07e-05 (-0.026)	0.478 (0.997)	0.0598	-0.0122 (-0.104)
dd3	-0.00071 (-0.316)	-0.0111 (-0.261)	-0.0276 (-0.995)	0.0205 (0.077)	0.00307 (0.092)	0.0643 (0.214)	-0.00523 (-0.007)	7.66e-05 (0.046)	3.77e-05 (0.046)	-0.0833 (-0.089)	-0.0122 (-0.104)	0.23

## Models Comparison

Particle	$\chi^2_{R\chi T}/dof$	$\chi^2_{\chi R\chi T}/dof$	$\chi^2_{C_2^1}/dof$	$\chi^2_{C_2^2}/dof$
$\pi^0$	33.3/39	58.2/40	234.0/40	35.18/38
$\eta$	47.7/27	61.6/29	63.0/31	44.9/29
$\eta'$	50.3/36	208.5/38	42.39/40	33.6/38

Our best fit and its chiral limit are compared to the results obtained using updated and extended versions of CA. In the  $C_2^1$ , case we obtained  $a_{P,1,1} = 0.0048(9), 0.75(13), 2.677(25)$  for  $P = \pi^0, \eta, \eta'$ , respectively.

## Difference between $R\chi T$ approaches

JHEP 03 (2023) 118	This work
Ansätze	Computation from the $R\chi T$ Lagrangian
3 resonance multiplets	2 resonance multiplets
Chiral Limit	Chiral symmetry breaking up to $\mathcal{O}(m_P^2)$
Only $\pi^0$ ( $\chi L$ works well)	$\pi^0, \eta, \eta'$
More subleading OPE constraints	Only $\delta_\pi$ as subleading OPE constraint
2019 Lattice data PRD 100 (2019) 3, 034520	2023 Lattice data arXiv:2305.0457
Only $\pi^0$ LQCD data used	BaBar $\pi^0$ data not used

Summary of the main differences between our study and a chiral limit model with 3 vector meson resonance multiplets.